Thermoflow Multiplicity in a Cooled Tube

The coupling between the momentum and energy balances and the change of physical properties with temperature can give rise to situations in which the pressure drop vs. flow rate curve is nonmonotonic. This can lead to thermoflow multiplicity—the existence of different flow rates in a tube under the same overall pressure drop. A two-dimensional model is used to analyze the conditions leading to thermoflow multiplicity for an incompressible non-Newtonian fluid flowing in a cooled tube. First, the multiplicity features of various limiting models are determined. These results are later used to gain an understanding of the asymptotic multiplicity features of the general model. The results show that the temperature sensitivity of the viscosity necessary for thermoflow multiplicity to occur decreases with increasing Brinkman number or β (modified Stanton number), or with decreasing cooling temperature, Biot number, or power law parameter. Multiple flow rates for a prescribed pressure drop are unlikely to occur in heat exchangers in which the Brinkman numbers are usually low and Biot numbers are high but may be found in polymer processing applications.

Friedemann Stroh
Jorge Pita
Vemuri Balakotaiah
Dan Luss
Department of Chemical Engineering
University of Houston
Houston, TX 77204

Introduction

Thermoflow multiplicity refers to a situation in which different flow rates exist in a system under the same pressure drop. This phenomenon is caused by the coupling between the energy and momentum balances and the change of physical properties, such as fluid density or viscosity, with temperature or composition. The coupling is usually due to a heat generation or removal process such as a chemical reaction, viscous dissipation, or cooling of the tube.

For viscous flow in a tube, Kearsley (1962) was the first to find multiple flow rates for a given pressure drop using a one-dimensional model. Martin (1967) extended these results to a power law fluid. Pearson et al. (1973) and Shah and Pearson (1974a, b) assumed a uniform temperature at any axial cross section and showed that thermoflow multiplicity can occur when an incompressible fluid, the viscosity of which is very sensitive to temperature changes, is cooled in a heat exchanger. Merzhanov and Stolin (1974) assumed a constant radial temperature profile in the cooled tube and found that thermoflow multiplicity may occur for a Newtonian fluid flowing in a cooled tube. They determined the region of parameters in which the flow rate vs. pressure drop curve was single-valued. Davis et al. (1983) determined the influence of viscous dissipation on thermoflow multiplicity in a tube, using the model of Kearsley (1962). Thermoflow multiplicity is known to occur in polymer processing (Pearson, 1985).

Gupalo and Rayazantsev (1968) and Matros and Chumakova (1980) found that thermoflow multiplicity could occur in chemical reactors. Lee et al. (1987, 1988) and Pita et al. (1989) presented a detailed analysis of the conditions leading to this multiplicity in packed-bed reactors. These studies have shown that the main cause for thermoflow multiplicity in the reactors was the change of density with temperature. A qualitative explanation of the cause for multiplicity in multitube reactors was provided by Lee et al. (1987).

To gain a qualitative understanding of the cause of thermoflow multiplicity, consider a viscous fluid in a tube cooled from the outside. The entering hot fluid has a low viscosity. If it moves fast, it leaves the tube at a temperature close to that at the inlet. If it moves slowly, the fluid temperature decreases substantially along the tube and its viscosity increases. The viscosity increase further reduces the velocity. This positive feedback mechanism can lead to thermoflow multiplicity so that both the fast-moving

Correspondence concerning this paper should be addressed to V. Balakotaiah and D. Luss.

low-viscosity fluid and the slow-moving high-viscosity fluid lead to the same overall pressure drop. The initial conditions in the tube determine which of the steady states is obtained.

In this paper we analyze the conditions that lead to thermoflow multiplicity for an incompressible non-Newtonian fluid flowing in a cooled tube, using a two-dimensional model that accounts for both axial and radial temperature gradients, viscous dissipation, and heat removal by cooling. This model includes as special cases all previous literature models as well as other limiting cases not considered previously. We present maps of the parameter regions in which thermoflow multiplicity exists. A major concern of our analysis is the relation between the predictions of the general model and those of simplified limiting models, and an examination if and for what systems this behavior can occur under practical conditions.

Mathematical Model

We assume that when the fluid enters the cooled zone it has a fully developed laminar velocity profile and a constant temperature. Further, we assume that the velocity profile changes very slowly in the axial direction and that no radial pressure gradient exists, that axial conduction is negligible in comparison with axial convection, and that radial heat convection is negligible in comparison with radial conduction. (Radial convection is caused by the change in the axial velocity profile of the cooled fluid.) The validity of these assumptions is considered further in the conclusions section.

With the above assumptions, the momentum and energy balances are

$$\frac{dp}{dz} = \frac{1}{r}\frac{\partial}{\partial r}\left[\mu(T, n) r \frac{\partial v_z}{\partial r}\right] \tag{1}$$

$$\rho c_p v_z \frac{\partial T}{\partial z} = \frac{k}{r}\frac{\partial}{\partial r}\left(r\frac{\partial T}{\partial r}\right) + \mu(T, n)\left(\frac{\partial v_z}{\partial r}\right)^2 \tag{2}$$

We assume that the viscosity of the non-Newtonian fluid satisfies a power law (Ostwald–de Waele) relation and an exponential temperature dependency, that is:

$$\mu(T, n) = A \exp\left(\frac{B}{T}\right)\left|\frac{\partial v_z}{\partial r}\right|^{n-1} = \mu_0(T_0)\exp\left[\frac{B}{T_0}\left(\frac{T_0 - T}{T}\right)\right]\left|\frac{\partial v_z}{\partial r}\right|^{n-1} \tag{3}$$

We assume that the density change with temperature is much smaller than that of the viscosity. The associated boundary conditions are

$$p = p_0,\ T = T_0 \quad \text{at } z = 0 \tag{4a}$$

$$p = p_L \quad \text{at } z = L \tag{4b}$$

$$\frac{\partial v_z}{\partial r} = 0,\ \frac{\partial T}{\partial r} = 0 \quad \text{at } r = 0 \tag{4c}$$

$$v_z = 0,\ -k\frac{\partial T}{\partial r} = h(T - T_w) \quad \text{at } r = R \tag{4d}$$

We define the following dimensionless variables

$$x = \frac{z}{L} \qquad \xi = \frac{r}{R} \qquad y = \frac{T}{T_0}$$

$$\pi = \frac{p}{p_0} \qquad u = \frac{v_z}{u^*}$$

$$X(y) = \exp\left(\frac{\gamma}{y} - \gamma\right) \qquad \gamma = \frac{B}{T_0} \tag{5a}$$

and the characteristic times

$$t_h = \frac{R\rho c_p}{h} \qquad t_R = \frac{R^2\rho c_p}{k}$$

$$t_c = \frac{2L}{u^*} \qquad t_\mu = \frac{\rho c_p T_0}{\mu_0}\left(\frac{R}{u^*}\right)^{n+1} \tag{5b}$$

t_h is the characteristic time for heat transfer through the wall, t_R is the characteristic time for radial conduction, t_c is the characteristic time for axial convection, and t_μ is the characteristic time for viscous heat generation. The smaller a characteristic time, the faster is this process.

The function $X(y)$ describes the sensitivity of the viscosity to changes in the temperature, which increases as the dimensionless parameter γ increases. To obtain simple dimensionless equations, we select the characteristic velocity u^* to be

$$u^* = \left(\frac{p_0 R^{n+1}}{8L\mu_0}\right)^{1/n} \tag{6}$$

The characteristic velocity itself has no physical meaning. However, it is related to the average velocity $v_{z,av}$ in a tube with a pressure drop p_0 and constant properties by the expression

$$v_{z,av} = \frac{n}{3n+1} 4^{1/n} u^* \tag{7a}$$

To get a relation between the general average velocity in the tube (with any pressure drop and not constant properties) and the characteristic velocity u^* we define the dimensionless average velocity U by the relation

$$U = 2\int_0^1 \xi u\, d\xi \tag{7b}$$

Using the above definitions, the momentum and energy balances become:

$$8\frac{d\pi}{dx} = \frac{1}{\xi}\frac{\partial}{\partial \xi}\left[X(y)\xi\frac{\partial u}{\partial \xi}\left|\frac{\partial u}{\partial \xi}\right|^{n-1}\right] \tag{8}$$

$$\frac{2u}{t_c}\frac{\partial y}{\partial x} = \frac{1}{t_R}\frac{1}{\xi}\frac{\partial}{\partial \xi}\left(\xi\frac{\partial y}{\partial \xi}\right) + \frac{1}{t_\mu}X(y)\left(\frac{\partial u}{\partial \xi}\right)^2\left|\frac{\partial u}{\partial \xi}\right|^{n-1} \tag{9}$$

The corresponding boundary conditions are:

$$y = 1,\ \pi = 1 \quad \text{at } x = 0 \tag{10a}$$

$$\pi = \pi_1 \quad \text{at } x = 1 \tag{10b}$$

$$\frac{\partial u}{\partial \xi} = 0, \frac{\partial y}{\partial \xi} = 0 \quad \text{at } \xi = 0 \tag{10c}$$

$$u = 0, \frac{1}{t_R}\frac{\partial y}{\partial \xi} + \frac{1}{t_h}(y - y_w) = 0 \quad \text{at } \xi = 1 \tag{10d}$$

We use dimensionless quantities, which are ratios of characteristic times, to transform Eqs. 9 and 10d into, respectively,

$$2u\frac{\partial y}{\partial x} = \frac{\beta}{Bi}\left[\frac{1}{\xi}\frac{\partial}{\partial \xi}\left(\xi\frac{\partial y}{\partial \xi}\right) + BrX(y)\left(\frac{\partial u}{\partial \xi}\right)^2\left|\frac{\partial u}{\partial \xi}\right|^{n-1}\right] \tag{11}$$

and

$$\frac{\partial y}{\partial \xi} + Bi(y - y_w) = 0 \quad \text{at } \xi = 1 \tag{12}$$

The new dimensionless parameters are the Biot number, Bi, the Brinkman number, Br, and β (a modified Stanton number), which are defined as

$$Bi = \frac{t_R}{t_h} = \frac{hR}{k}$$

$$Br = \frac{t_R}{t_\mu} = \frac{\mu_0 u^{*n+1}}{kT_0 R^{n-1}}$$

$$\beta = \frac{t_c}{t_h} = \frac{2hL}{Ru^*\rho c_p} \tag{13}$$

Equations 8, 11, and 7b with boundary conditions 10a–10c and 12 form the general model. The objective of this study is to determine the dependence of the flow rate (or equivalently U) on the pressure drop (or equivalently π_1) and the parameter values for which this curve is multivalued.

The solution is symmetric with respect to the center of the tube. Thus, using the transformation $\eta = \xi^2$ Eqs. 8 and 11 become

$$\frac{d\pi}{dx} = 2^{n-2}\frac{\partial}{\partial \eta}\left[X(y)\eta^{(n+1)/2}\frac{\partial u}{\partial \eta}\left|\frac{\partial u}{\partial \eta}\right|^{n-1}\right] \tag{14}$$

$$\frac{\partial y}{\partial x} = \frac{2\beta}{Biu}\left[\frac{\partial}{\partial \eta}\left(\eta\frac{\partial y}{\partial \eta}\right) + BrX(y)\,\eta^{(n+1)/2}\,2^{n-1}\left(\frac{\partial u}{\partial \eta}\right)^2\left|\frac{\partial u}{\partial \eta}\right|^{n-1}\right] \tag{15}$$

The corresponding definition of the average dimensionless velocity becomes

$$U = \int_0^1 u\,d\eta \tag{16}$$

Boundary conditions 10a and 10b remain unchanged but 10d and 12 are replaced by

$$u = 0, \frac{\partial y}{\partial \eta} + \frac{Bi}{2}(y - y_w) = 0 \quad \text{at } \eta = 1 \tag{17}$$

The symmetry boundary condition, Eq. 10c, at $\xi = 0$ is satisfied automatically.

Numerical Solution of Model

The above mathematical model was solved numerically using the collocation method to describe the radial derivatives and a finite-difference scheme for the axial derivatives. The velocity profile at any axial point was approximated by

$$u(\eta) = \sum_{k=1}^{N+1} a_k P_k(\eta) \tag{18}$$

where $P_k(\eta)$ are orthogonal polynomials (Villadsen and Michelsen, 1978) and a_k are constants to be determined. The number of radial collocation points, N, was usually four. Writing Eq. 14 for the N collocation points gives $N - 1$ conditions about the coefficients a_k. The other two conditions are obtained from the surface boundary condition and the Gauss-Jacobi quadrature relation for Eq. 16 (Villadsen and Michelsen, 1978):

$$U = \sum_{k=1}^{N+1} u_k w_k \tag{19}$$

Because the temperature profile may be very steep, an adequate description is not possible by a single polynomial, which tends to oscillate in such cases. Thus, it was described by collocation on finite elements (Finlayson, 1980), where the radial domain is split into M intervals using an Lth-order polynomial in each interval (in our case L was 2). Specifically, we used the representation

$$y(\eta) = \sum_{k=1}^{M+1}\sum_{L=1}^{2} b_{kL}P_{kL}(\eta) \tag{20}$$

where M was between 4 and 7. The value of y was computed by a finite-difference form of Eq. 15, starting at $x = 0$ and moving in the downstream direction to find the dimensionless exit pressure corresponding to the assumed U. Experience has shown that the number of collocation points has to be increased with a decrease in the value of the power law exponent n or an increase in the Brinkman number.

Repeating these calculations for a series of assumed U values using the continuation scheme of Kubicek and Marek (1983) enables the construction of a bifurcation diagram of π_1 vs. U. A typical example is shown in Figure 1. When U is a monotonic function of π_1, a unique inlet solution exists for any outlet pressure. When the graph is not monotonic (e.g., $\gamma = 10$ in Figure 1) several inlet velocities can exist for all outlet pressures between the ignition and extinction points. Increasing the temperature sensitivity parameter γ increases the range of exit pressures for which multiplicity occurs. The initial conditions and the stability of the solutions determine which of the solutions is reached. It can be shown that whenever three solutions exist, the intermediate one is always unstable.

Figures 2 and 3 describe the axial pressure and average temperature profiles for the three different flow rates U with $\pi_1 = 0.8$. Figure 3 shows that the higher the average velocity, the smaller is the average temperature change in the axial direction.

The general model contains six parameters: γ, β, Bi, Br, y_w, n. When the values of five of these are specified, the multiplicity region in the plane of the remaining parameter and π_1 is bounded by the loci of the ignition and extinction points, each of

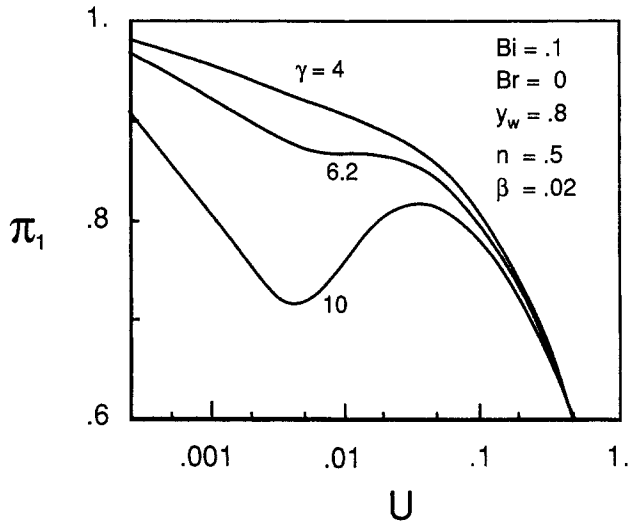

Figure 1. Typical bifurcation diagrams of exit pressure vs. flow rate (velocity) for three γ values.

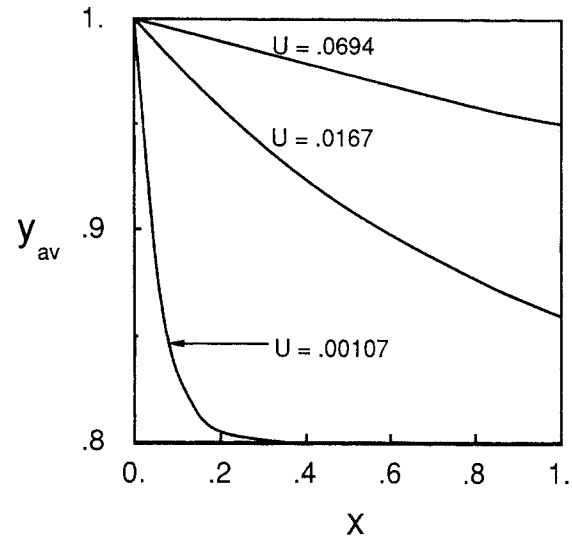

Figure 3. Average temperature profiles of the three states that exist under the same overall pressure drop.
Parameters as in Figure 2.

which satisfies both the steady-state equation

$$F(U, \pi_1, \gamma, \beta, Bi, Br, y_w, n) \equiv \pi(1, U) - \pi_1 = 0 \quad (21)$$

and

$$\frac{dF}{dU} = 0 \quad (22)$$

Elimination of U from Eqs. 21 and 22 gives the bifurcation set in the parameter space. A cross section of this set is shown in the π_1, γ plane in Figure 4.

The loci of the ignition and extinction points coalesce at a cusp point, Figure 4. A unique solution exists for all γ values smaller than that of the cusp point, at which

$$F = \frac{dF}{dU} = \frac{d^2F}{dU^2} = 0 \quad (23)$$

The method of Witmer et al. (1986) was used to find the cusp points of this two-point boundary value problem. Appendix A describes the application of that procedure to this problem. Again the continuation scheme of Kubicek and Marek (1983) was used to construct the loci of these points. The calculations indicate that a cusp point is the singular point of the highest co-dimension of this model, suggesting that at most three solutions exist for any parameter set.

It is important to know the range of practical values of the six parameters in the model. In most applications, the Biot number

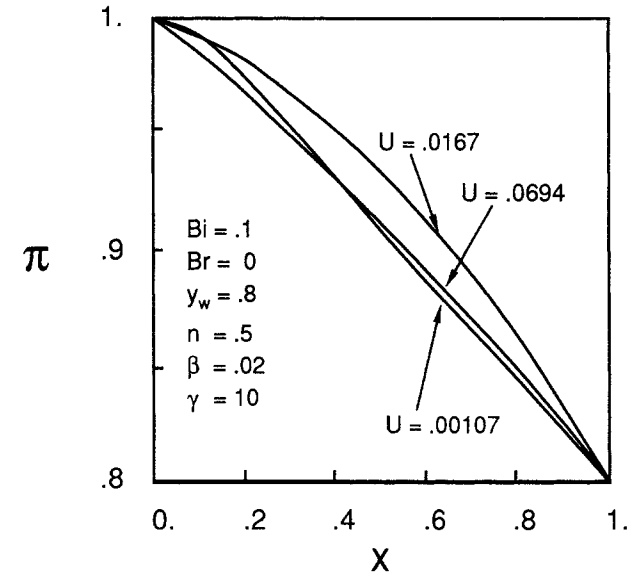

Figure 2. Pressure profiles of three states that exist under the same overall pressure drop.

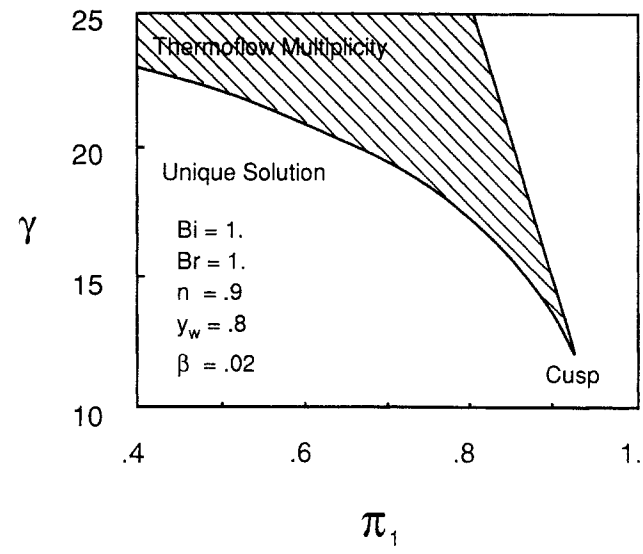

Figure 4. Multiplicity region in γ, π_1 plane.

is in the range 0.01 to 10. The Brinkman number is usually very small, of the order of 0.0001. Only in viscous polymer processing it may be of order 1 or even more. The value of β is usually between 0.0001 and 1.0. For most Newtonian fluids γ has values between 5 and 30. For example, for water $\gamma = 5.9$, phenol $\gamma = 9.2$, light machine oil $\gamma = 10.7$, heavy machine oil $\gamma = 21.4$, and for glycerin $\gamma = 26.9$. For low-density polyethylene γ is between 8 and 17 (Meissner, 1971). The value of y_w normally varies from 0.7 to 0.95. For Newtonian fluids $n = 1$, and for polymers n may be as small as 0.3. As our base case, we selected the parameter values to be $\beta = 0.02$, $Br = 0$, $Bi = 1.0$, and $y_w = 0.8$.

Analysis of Simplified Models

Prior to the discussion of the general model, we analyze in this section some simplified limiting models. These models are useful for gaining insight and understanding of the asymptotic behavior of the general model. The simplified models are obtained when one characteristic time in Eqs. 9 and 10d is either very large or very small compared with the other characteristic times.

Constant wall temperature model

The first simplified model we consider is the case of $t_h \to 0$, for which the heat transfer through the wall is very large. This changes the boundary condition of the general model, Eq. 17, to

$$y = y_w \quad \text{at } \eta = 1 \tag{24}$$

It follows from Eq. 13 that for $t_h \to 0$, $Bi \to \infty$ and $\beta \to \infty$, but the ratio Bi/β is finite. Therefore, the parameters of the constant wall temperature model are Bi/β and Br, besides n, y_w, and γ. This limiting model is valid for large values of Bi and β and provides an asymptote for the cusp points of the general model in the Bi, β plane. Figure 5 shows the locus of the cusp points of this model in the plane of Bi/β vs. Br. For each fixed y_w, n, and γ the cusp locus divides the plane into two regions. The dependence of the flow rate on the pressure drop is single-valued in the region above the graph and multivalued in the other region. The hysteresis curves have a vertical asymptote at the origin, implying that this model does not show multivalued behavior in the limit of $t_R \to 0$. The reason for this is that in this case the temperature at the tube remains constant at y_w. The region of uniqueness for this model, as well as for all the other models, increases with increasing y_w and n and decreasing γ values.

Insulated tube model

The limiting case of $t_h \to \infty$ corresponds to situations in which the rate of heat transfer through the wall is very small, that is, the tube is insulated. Here, boundary condition 17 of the general model is replaced by

$$\frac{\partial y}{\partial \eta} = 0 \quad \text{at } \eta = 1 \tag{25}$$

This insulated tube model is valid for $Bi \to 0$ and $\beta \to 0$ with a finite ratio of Bi/β. This model predicts the asymptote of the cusp points of the general model in the Bi, β plane for small values of Bi and β, if such an asymptote exists. We were unable to find any cusp points for this model (we also had numerical problems for large U). However, we are also unable to prove that this model always has a unique solution. We show in Appendix B that multiplicity is not possible for the special case of $\beta/Bi \to \infty$. Figure 6 describes some numerically calculated bifurcation diagrams for this model. The graphs for finite values of β/Bi lie above the limiting graph for $\beta/Bi \to \infty$ but there is no indication of multiplicity. For reasons explained later, the special case with $\beta/Bi \to \infty$ is called the insulated tube with constant radial temperature model.

Constant radial temperature model

The third limiting case we consider is of $t_R \to 0$, for which the conduction in the radial direction is very high and the radial temperature profile is essentially uniform. When y, and therefore $X(y)$ are independent of η, the momentum balance can be written as

$$\frac{2^{2-n}}{X(y)}\frac{d\pi}{dx} = \frac{\partial}{\partial \eta}\left(\eta^{(n+1)/2}\frac{\partial u}{\partial \eta}\left|\frac{\partial u}{\partial \eta}\right|^{n-1}\right) = C_1 \tag{26}$$

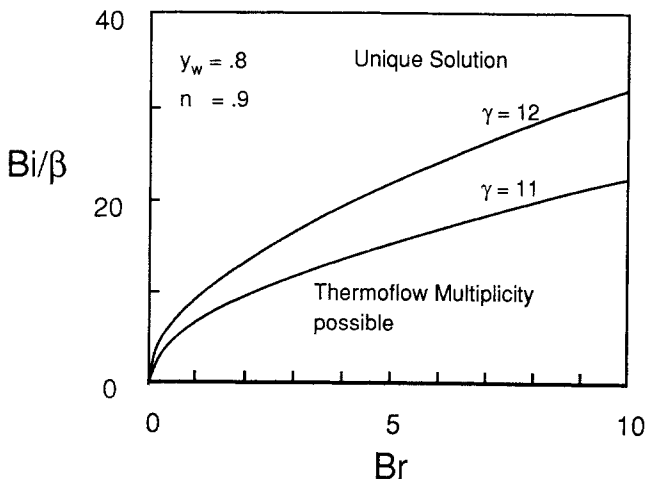

Figure 5. Locus of cusp points, constant wall temperature model.

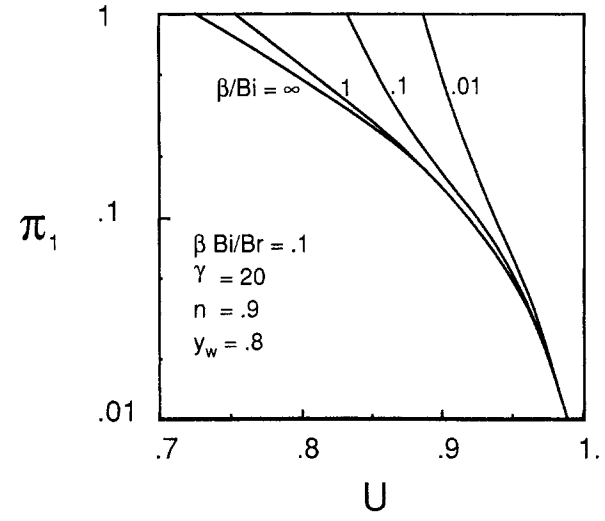

Figure 6. Bifurcation diagrams of π_1 vs. U, insulated tube model.

The lefthand side of Eq. 26 depends on x and the righthand side only on η. Therefore, each side is equal to a constant. Solving the righthand side we get

$$u = C_1^{1/n} \frac{2n}{1+n} [\eta^{(1+n)/2n} - 1] \tag{27}$$

The constant C_1 is determined by using the definition for U, Eq. 16. The lefthand side of the momentum balance then gives

$$\frac{d\pi}{dx} = -X(y)2^{n-2}\left(\frac{1+3n}{2n}\right)^n U^n \tag{28}$$

To remove the η dependence from the energy balance we integrate it in the radial direction to obtain, after use of boundary condition 17,

$$\frac{dy}{dx} = -\frac{\beta}{U}(y - y_w) + \frac{\beta\, BrX(y)2^n}{Bi} U^n \left(\frac{1+3n}{2n}\right)^n \tag{29}$$

Thus, this simplified model consists of two ordinary differential equations. The boundary conditions in the axial direction are the same as for the complete model. Merzhanov and Stolin (1974) have analyzed this limiting model for a Newtonian fluid. Pearson et al. (1973) and Shah and Pearson (1974a, b) have used it to analyze the flow between two parallel plates with a simplified temperature dependence of the viscosity (positive exponential approximation). Using linear stability analysis, they determined the marginal stability boundaries in a plane of two parameters. However, one of these parameters, the Graetz number, depends on the unknown velocity U. Our maps do not require the specification of the velocity.

It follows from Eq. 13 that this model is valid for $Bi \to 0$ and $Br \to 0$ with a finite ratio of Bi/Br. Thus, instead of the parameters Bi and Br this constant radial temperature model contains only Bi/Br. It can be used to generate an asymptote of the cusp points of the general model in the Bi, Br plane.

Figure 7 describes the cusp locus of this model for three different values of n. The curves divide the parameter space into a region in which thermoflow multiplicity exists and one in which it cannot occur. (In all the following graphs, the multiplicity region is above the curve.) The locus of the cusp points for the constant radial temperature model has two constant asymptotes for $Bi/Br \to 0$ and $Bi/Br \to \infty$. The region of multiplicity decreases with increasing Bi/Br between the two limiting asymptotes. These asymptotes correspond to two further simplified models, the infinite tube with constant radial temperature model for $Bi/Br \to 0$, and the constant radial temperature with no dissipation model for $Bi/Br \to \infty$. We discuss these limiting models later.

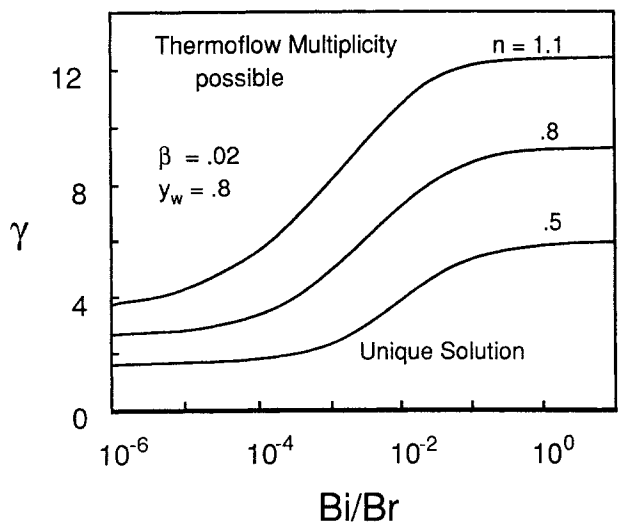

Figure 7. Dependence of γ at cusp point on Bi/Br, constant radial temperature model.

The other limiting case, of $t_R \to \infty$, for which nearly no conduction exists in the radial direction, gives no new simplified model. Similarly, the case of $t_c \to 0$, for which the residence time is very short, does not simplify the analysis of the general model.

Infinite tube model

The limiting case of $t_c \to \infty$ is one for which the temperature profile does not change in the axial direction because the residence time in the tube is very large so that an equilibrium state is reached. With this assumption, Eq. 11 is reduced to

$$\frac{1}{\xi}\frac{\partial}{\partial\xi}\left(\xi\frac{\partial y}{\partial\xi}\right) + BrX(y)\left(\frac{\partial u}{\partial\xi}\right)^2\left|\frac{\partial u}{\partial\xi}\right|^{n-1} = 0 \tag{30}$$

Integrating the momentum balance, Eq. 8, first with respect to x from 0 to 1 and then with respect to ξ, we get

$$4\,\xi(\pi_1 - 1) = X(y)\frac{\partial u}{\partial\xi}\left|\frac{\partial u}{\partial\xi}\right|^{n-1} + C_2 \tag{31}$$

Using boundary condition 10c we find that the constant C_2 is zero, so that Eq. 31 can be rewritten as

$$\left|\frac{\partial u}{\partial\xi}\right| = \left[\frac{4\xi(1-\pi_1)}{X(y)}\right]^{1/n} \tag{32}$$

Substitution of Eq. 32 in Eq. 30 gives

$$\frac{1}{\xi}\frac{d}{d\xi}\left(\xi\frac{dy}{d\xi}\right) + \Lambda\xi^{1+1/n}\exp\left(\gamma^* - \frac{\gamma^*}{y}\right) = 0 \tag{33a}$$

where

$$\Lambda = Br(4(1-\pi_1))^{1+1/n} \text{ and } \gamma^* = \frac{\gamma}{n} \tag{33b}$$

The corresponding boundary conditions are Eqs. 10c and 12. Equations 33 and 12 show that the γ value at the cusp point will depend on n, Bi, and y_w but not on the value of Br.

This infinite tube model is valid for $\beta \to \infty$, while Bi is finite. It predicts the asymptotic cusp points of the general model in any plane with β in one axis and a parameter (other than Br) in the other axis.

Figure 8 describes the cusp locus of this model. There are two asymptotes for large and small values of Bi. Again the asymptotes can be described by more simplified models, the infinite tube with constant radial temperature model for small Bi, and the infinite tube with constant wall temperature model for large

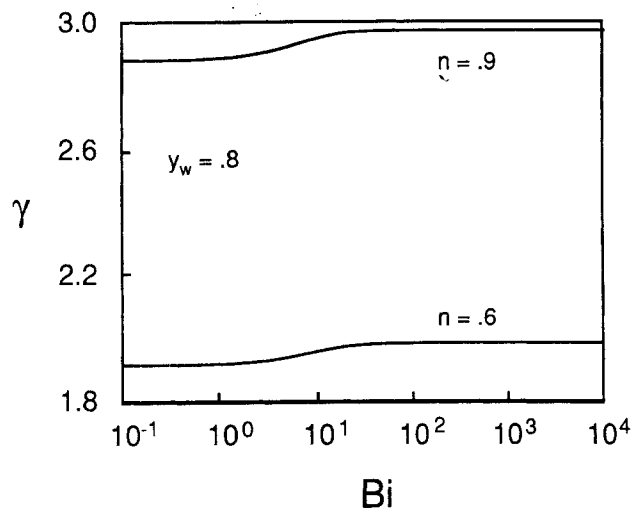

Figure 8. Dependence of γ at cusp point on *Bi*, infinite tube model.

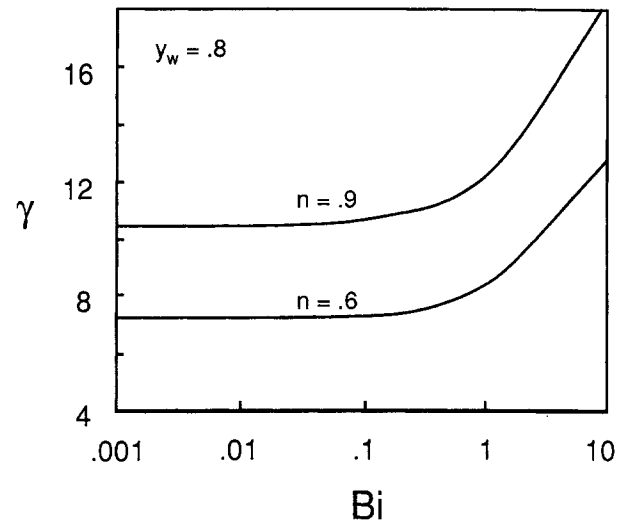

Figure 9. Dependence of γ at cusp point on *Bi*, no-dissipation model.

Bi, which we discuss later. At intermediate *Bi* values the value of the minimal γ, for which thermoflow multiplicity can occur, increases with increasing values of *Bi*.

Negligible dissipation model

The limiting case of $t_\mu \to 0$ means that the heat generation is the dominant term so that the fluid temperature increases rapidly without any limit (at least in theory). Therefore, this assumption does not lead to any simplified model. But for the limiting case of $t_\mu \to \infty$ the viscous dissipation is negligible and Eq. 11 is reduced to

$$2u\frac{\partial y}{\partial x} = \frac{\beta}{Bi}\frac{1}{\xi}\frac{\partial}{\partial \xi}\left(\xi\frac{\partial y}{\partial \xi}\right) \tag{34}$$

For this limiting no-dissipation model we can define new variables in Eqs. 8 and 34. We can combine u/β in Eq. 34 to a new $\hat{u}$ and in Eq. 8 we define a $\hat{\pi}$ as π/β^n. Thus, β influences only the values of U and π_1 for which thermoflow multiplicity occurs but not the region of multiplicity in the space of the remaining parameters. This model is valid for $Br \to 0$, and gives the asymptotic cusp points of the general model in a plane with *Br* in one axis and a parameter (other than *Bi*, because t_R has to be finite) in the other axis. Figure 9 describes the cusp points of this limiting model. For small *Bi* values there exists an asymptotic γ value below which multiplicity does not exist. As *Bi* increases this limiting γ value increases without limit. The asymptote for $Bi \to 0$ is that of a more simplified constant radial temperature with no dissipation model, discussed later.

Additional simplified models

In all the limiting models discussed so far, the number of parameters is reduced by one from six to five. The figures of the cusp locus of the limiting models show that there exist further simplified models that describe the asymptotic behavior of the limiting models. These models are obtained if two characteristic times have extreme values or equivalently by combining two of the limiting models discussed above. Not all combinations are possible, but we get five more models.

The first combination is of $t_h \to 0$, that is, the constant wall temperature model with $t_c \to \infty$, which is the infinite tube model. This model is valid for $Bi \to \infty$, $\beta \to \infty$, and $Bi/\beta \to 0$. This simplified infinite tube with constant wall temperature model contains only the parameter *Br* besides *n*, y_w, and γ. This model was solved by Kearsley (1962) and Martin (1967) using a simplified temperature dependence of the viscosity. Davis et al. (1983) used this asymptotic model to show that thermoflow multiplicity exists for a Newtonian fluid.

The next possible combination is of $t_\mu \to \infty$ with $t_h \to 0$, that is, of the no-dissipation model, Eq. 34, with the constant wall temperature boundary condition, Eq. 24. This model is valid for $Bi \to \infty$, $\beta \to \infty$, $Br \to 0$, and Bi/β finite. As for the no-dissipation model, we can combine the parameter Bi/β with the variables π and u. The cusp points therefore depend only on *n*, y_w, and γ. For constant viscosity, this constant wall temperature with no dissipation model is the classical Graetz problem.

The case of $t_R \to 0$ and $t_h \to \infty$ combines the constant radial temperature model, Eqs. 28, 29, with the insulated tube boundary condition. Because of the new boundary condition Eq. 29 is replaced in this model by

$$\frac{dy}{dx} = \frac{\beta Br X(y) 2^n}{Bi} U^n \left(\frac{1+3n}{2n}\right)^n \tag{35}$$

but Eq. 28 remains unchanged. In this insulated tube with constant radial temperature model $Bi \to 0$, $Br \to 0$, $\beta \to 0$, $Bi/Br \to 0$, and $Bi/(Br\,\beta)$ is finite. It is proved in Appendix B that this model cannot have multiplicity.

Combining the constant radial temperature model ($t_R \to 0$) with the infinite tube model ($t_c \to \infty$) gives the infinite tube with constant radial temperature model. Here the average velocity and temperature satisfy the equations

$$\pi_1 = 1 - X(y)2^{n-2}\left(\frac{1+3n}{2n}\right)^n U^n \tag{36}$$

$$\frac{BrX(y)2^n}{Bi} U^{n+1}\left(\frac{1+3n}{2n}\right)^n - (y - y_w) = 0 \tag{37}$$

Dividing Eq. 36 by Eq. 37 we get

$$4U(1 - \pi_1) = \frac{Bi}{Br}(y - y_w) \tag{38}$$

Solving Eq. 38 for U and substituting this value in Eq. 36 gives

$$\frac{\exp\left(\gamma - \frac{\gamma}{y}\right)}{(y - y_w)^n} = \Phi \tag{39a}$$

where

$$\Phi = \frac{\left(\frac{1 + 3n}{2n}\frac{Bi}{Br}\right)^n}{2^{n+2}(1 - \pi_1)^{n+1}} \tag{39b}$$

The cusp points of Eq. 39a are at

$$\gamma = 4ny_w$$
$$y = 2y_w$$
$$\Phi = \frac{\exp(4ny_w - 2n)}{y_w^n} \tag{40}$$

Figures 7 and 8 show how this limiting γ value is reached asymptotically. This model is valid for $Bi \to 0$, $Br \to 0$, $\beta \to \infty$, and Bi/Br is finite.

Finally, we can combine the constant radial temperature model ($t_R \to 0$) with the no-dissipation model ($t_\mu \to \infty$) to get the constant radial temperature with no dissipation model. It satisfies Eq. 28 and

$$\frac{dy}{dx} = -\frac{\beta}{U}(y - y_w) \tag{41}$$

The solution of Eq. 41 with boundary condition 10a is

$$y = y_w + (1 - y_w)\exp\left(-\frac{\beta x}{U}\right) \tag{42}$$

Using this explicit expression for $y(x)$ we can integrate Eq. 28 to get

$$\pi_1 = 1 - \int_0^1 X[y(x)]2^{n-2}\left(\frac{1 + 3n}{2n}\right)^n U^n\, dx \tag{43}$$

This model is valid for $Bi \to 0$, $Br \to 0$, and $Bi/Br \to \infty$. As for the no-dissipation model, we can combine the variables with the parameter β, and the cusp points depend only on n, y_w, and γ.

All other combinations give trivial solutions or lead to contradictions. It is obvious that $t_h \to 0$ (constant wall temperature model) and $t_h \to \infty$ (insulated tube model) cannot occur at the same time. If we combine the constant wall temperature model with the constant radial temperature model the temperature at all points in the tube is y_w. This trivial model is the limiting case in Figure 5 for small Bi and Br. Thermoflow multiplicity does not exist in this case. The insulated tube model and the infinite tube model cannot be combined because it is not possible to get an equilibrium state without heat removal unless the Brinkman number is zero (no dissipation model). The combination of the no dissipation model with the insulated tube model is the trivial case of isothermal flow in a tube. Finally, it is not possible to combine the infinite tube model and the no-dissipation model because it gives only the trivial solution of $y = y_w$ everywhere.

Table 1. Characteristic Times Corresponding to the Various Simplified Models

Model	t_h	t_R	t_c	t_μ
Constant wall temperature	0	1	1	1
Insulated tube	∞	1	1	1
Constant radial temperature	1	0	1	1
Infinite tube	1	1	∞	1
No dissipation	1	1	1	∞
Infinite tube with constant wall temperature	0	1	∞	1
Constant wall temperature with no dissipation	0	1	1	∞
Insulated tube with constant radial temperature	∞	0	1	1
Infinite tube with constant radial temperature	1	0	∞	1
Constant radial temperature with no dissipation	1	0	1	∞
Isothermal $y = y_w$	0/1	0/1	$1/\infty$	$1/\infty$
Isothermal $y = 1$	∞	1	1	∞

The above five new combined models have two parameters less than the complete model. Table 1 summarizes all the possible models. For each limiting case, the table shows only one combination of characteristic times. There may be other combinations that also give this asymptotic model. One example is the case of $t_h \to \infty$, $t_R \to \infty$, $t_\mu \to \infty$, and $t_c = 1$, which corresponds to the no-dissipation model.

The above limiting models may be used to predict multiplicity in a variety of other problems in which mechanisms different from external cooling lead to changes in the physical properties of the fluid.

Thermoflow Multiplicity Analysis for the General Model

In this section we analyze the influence of all the parameters on the region in which thermoflow multiplicity is possible. The parameter γ contains only fluid properties and we shall determine the minimal value this parameter needs to have so that thermoflow multiplicity can occur for some π_1 as a function of the other model parameters. In all the figures to be shown, thermoflow multiplicity can occur only for γ values above the cusp loci. We shall use the simplified limiting models to gain insight into the behavior of the general model and to predict its asymptotic features.

Figure 10 shows the influence of β on the cusp locus. Very large values of β are not realistic, but to show both asymptotes we extended the graph to such large values. With increasing β thermoflow multiplicity can be found for smaller γ values. For very small and very large β the values of Br do not affect the limiting value of γ. Large Brinkman numbers shift the region of multiplicity to smaller γ values. A surprising result is that the critical γ is independent of β for $Br = 0$. We now try to explain

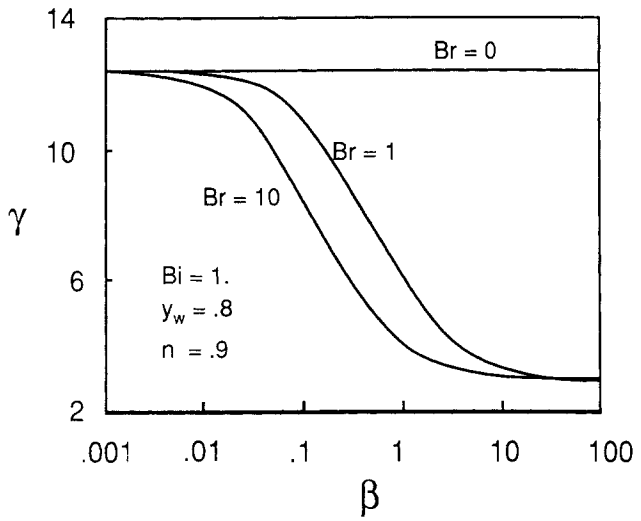

Figure 10. Dependence of γ at cusp point on β and *Br*, general model.

most of these features using the limiting models. We note that $\beta \to 0$ implies that $t_h \to \infty$. Since $t_h \to \infty$ and both Bi $(=t_R/t_h)$ and Br $(=t_R/t_\mu)$ are finite, it follows that $t_\mu \to \infty$ and $t_R \to \infty$. Equation 10d shows that if both t_h and t_R are unbounded, the general model does not reduce to the limiting insulated tube case. Only $t_\mu \to \infty$ simplifies the model. Thus, $\beta \to 0$ corresponds to the no-dissipation model. This is verified by Figure 10 as the curves for different Brinkman numbers coalesce for small values of β. For the case of $\beta \to \infty$ we get $t_c \to \infty$, the infinite tube model, where the value of γ at the cusp point depends on Bi only. Therefore, all the curves for different Br coalesce again. A special case is $Br = 0$, the no-dissipation model (valid now for all values of β). As explained above, the γ values of the cusp points of this case are independent of β.

Figure 11 shows the influence of the Biot number on the value of γ at the cusp point. Increasing the Biot number shifts the locus of the cusp points to larger γ values. Unless $Br = 0$ the curves do not reach a constant limiting γ value for small Bi within the graph. For large Bi the curves for different Brinkman numbers coalesce. We look again at the characteristic times to find limiting models that explain the observed features. The limiting model for small Biot and Brinkman numbers is the constant radial temperature model with $t_R \to 0$. This model contains instead of Bi and Br only the ratio Bi/Br. For $Br = 0$ the value of $Bi/Br \to \infty$ and Figure 7 shows that a finite limiting γ value exists in this case, which is the asymptote of the constant radial temperature with no dissipation model. Therefore, a horizontal γ asymptote exists for $Br = 0$ and small Biot numbers. For finite Brinkman numbers the ratio Bi/Br decreases for decreasing Biot numbers. Figure 7 shows that for decreasing Bi/Br the region of multiplicity begins at smaller γ values. Therefore, the γ values for $Br = 0.1$ decrease with decreasing Bi in Figure 11 and do not reach a limiting value as the case $Br = 0$. Finally, when $Bi/Br \to 0$, the γ asymptote of the infinite tube with constant radial temperature model is obtained. The cusp locus for $Br = 10$ cannot be described by a limiting model for small Bi, because Br is not small. But the qualitative behavior for $Br = 10$ follows that of the constant radial temperature model. For large Biot numbers we get the asymptote of the no-dissipation model with $t_\mu \to \infty$. Therefore, all the curves in Figure 11 with different Brinkman numbers coalesce for large Bi.

Figure 12 shows the influence of the Brinkman number on the γ values at the cusp points. Increasing Br decreases the γ value of the cusp points, that is, it expands the region of multiplicity. For very small and very large values of Br the cusp points occur at a limiting γ value. For small Br the viscous dissipation is negligible and the limiting model is the no-dissipation model, which is independent of Br. Therefore, the γ value at the cusp points reaches an asymptotic value for decreasing Br. For very large values of Br the limiting model is the infinite tube model where the cusp points are independent of Br.

Figure 13 shows that a nearly linear relationship exists between the power law parameter n and γ. Decreasing n reduces the γ values of the cusp point. An exact linear relation between γ and n is obtained for the infinite tube with constant radial temperature model, where the cusp points can be determined analytically.

The value of y_w has, in general, the strongest influence on the

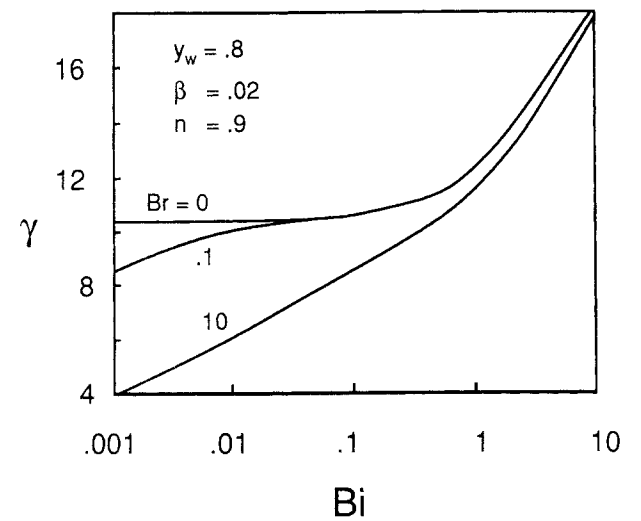

Figure 11. Dependence of γ at cusp point on *Bi* and *Br*, general model.

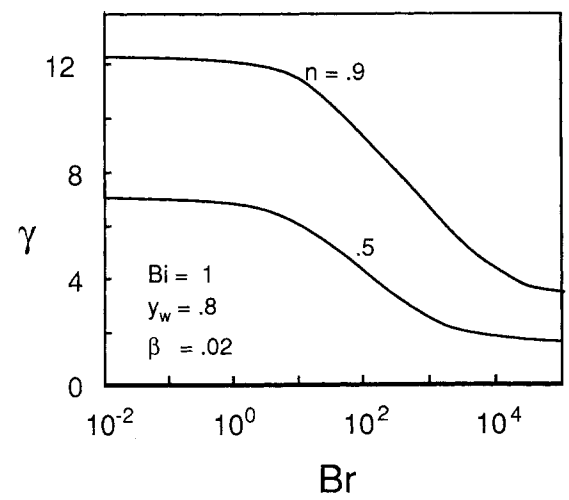

Figure 12. Dependence of γ at cusp point on *Br* and *n*, general model.

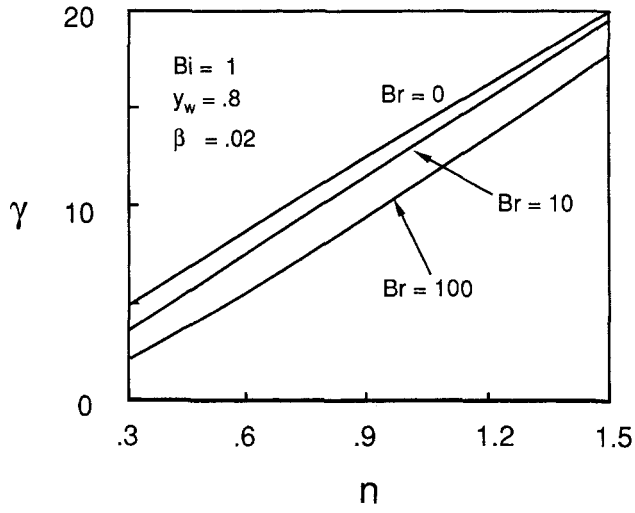

Figure 13. Dependence of γ at cusp point on n and Br, general model.

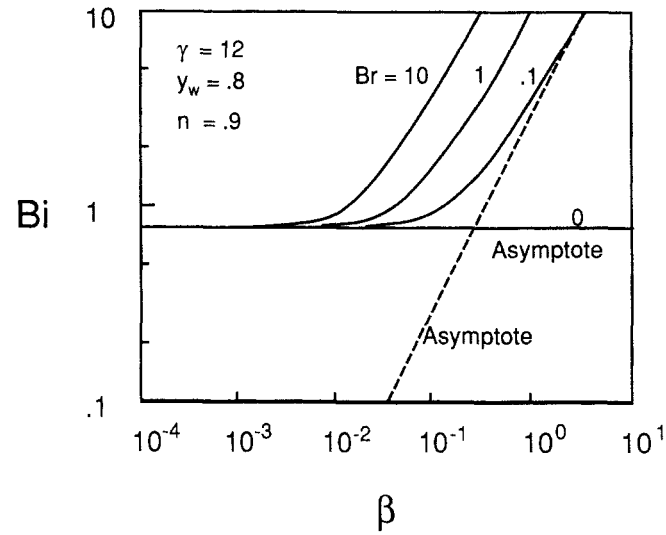

Figure 15. Cusp locus of general model in β, Bi plane for various Br values.

γ value at the cusp point unless we are close to the infinite tube asymptote. The graph of the cusp points, Figure 14, shows a pole close to $y_w = 1$. For y_w close to unity thermoflow multiplicity is not found for real fluids because the corresponding γ value is unrealistically large. But for decreasing y_w values, the γ value at the cusp point decreases rapidly to realistic values. Thus, a small change of y_w can cause a large change in the region of multiplicity. This is not surprising because y_w determines the magnitude of the heat removal, which is the main reason for temperature changes unless Br is very large. This also explains why the curves for different Br coalesce for small y_w, because the dissipation becomes less important when the cooling increases. If we are in the parameter region of the infinite tube asymptote, multiplicity is possible even for values of y_w larger than one.

We can sometimes use the limiting models to construct the cusp points of the general model. Figure 15 shows the cusp points in the β, Bi plane, for fixed values of γ, y_w, and n. Thermoflow multiplicity here is found for parameters below the curves.

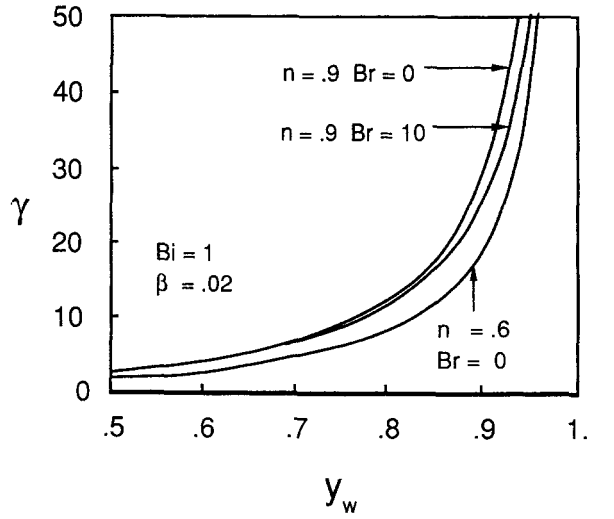

Figure 14. Dependence of γ at cusp point on y_w and n, general model.

For small values of β the asymptote has a constant Bi value for all Br. The value of Bi at the cusp points increases with increasing β except when $Br = 0$. For higher Br the increase in the Bi values starts at lower β values. For large β (or Bi) all the curves reach a slope of 1 when logarithmic scales are used.

The limiting model of small β with finite Bi and Br is the no-dissipation model. In that model γ at the cusp point depends on Bi. The limiting value of Bi as a function of the fixed parameter γ can be found from Figure 9. (If γ is lower than a limiting value, no limiting Bi exists.) The limiting model for large Bi and β is the constant wall temperature model, for which Figure 5 determines the dependence of Bi/β on Br at the cusp point. In the logarithmic graph of Bi vs. β any value of Bi/β is represented by a straight line of slope one. Hence, we can use Figure 5 to construct the asymptotes in Figure 15 for large β and Bi for any Br. Figure 15 shows that the two asymptotes give a good approximation of the cusp point locus for the complete model.

Conclusions

The conditions leading to thermoflow multiplicity for an incompressible non-Newtonian fluid flowing in a cooled tube were determined. The two-dimensional model analyzed here includes all the previously studied models as special cases. The occurrence of thermoflow multiplicity was determined first for various limiting models. The systematic approach of formulating these limiting (simplified) models and relating them later to the asymptotic behavior of the general model should be useful in many other applications.

The maps of multiplicity regions indicate that thermoflow multiplicity is very unlikely to occur in common heat exchangers. Most common Newtonian fluids have a low γ value. Moreover, heat exchangers are characterized by high Biot numbers and low Brinkman numbers, which again lead to uniqueness. Multiplicity is possible only for very high temperature differences in the heat exchanger (small y_w). It may occur for usual temperature differences only when a highly viscous fluid flows in a heat exchanger. These cases seem to be of no practical significance.

In polymer processing, viscous dissipation is very high and the

Brinkman number may be of order one or more. Moreover, the power law parameter n is usually much smaller than unity and γ exceeds 10. Thus, for typical y_w and π_1 values, thermoflow multiplicity may occur. In such cases, the exact region of multiplicity can be determined by constructing a bifurcation set as shown in Figure 4.

In the formulation of the momentum and energy balances, Eqs. 1 and 2, it is assumed that the velocity profile changes slowly in the axial direction (i.e., $\rho\, v_z\, \partial v_z/\partial z$ is very small compared to the pressure gradient). This assumption is always valid for the constant radial temperature and the infinite tube models. Thus the predictions of these models are valid for all values of the Reynolds number for which the flow remains laminar. For the general model, the assumption that $\partial v_z/\partial z \ll 1$ may not be satisfied if Bi or Br is large. In this case the predictions of the general model may be valid only if the Reynolds number is small (creeping flow). Unfortunately, it is not possible to estimate a priori the largest Reynolds number for which the predictions of the general model remain valid, and this value depends on the other parameters that characterize the system.

This work ignores the variation of density with temperature. Inclusion of this effect is expected to increase the range of parameters for which thermoflow multiplicity occurs. The approach presented here may be used to analyze that problem. We also ignore in this work the possible occurrence of oscillatory flows or symmetry breaking, leading to flow profiles that are not axisymmetric.

Acknowledgment

The authors are thankful for support of this research by the National Science Foundation, the Welch Foundation, and the Texas Advanced Research Program.

Notation

A = rheological parameter
B = rheological parameter
Bi = Biot number
Br = Brinkman number
C = constant
c_p = heat capacity
k = thermal conductivity
L = tube length
n = power law parameter
N = number of collocation points
p = pressure
P = polynomial
r = radial direction
R = radius of tube
T = temperature
u = dimensionless axial velocity
u^* = characteristic velocity
U = ratio of average velocity to characteristic velocity
v_z = axial velocity
$v_{z,av}$ = average velocity when $\pi(1) = 0$ and constant properties
x = dimensionless axial direction
$X = \exp(\gamma/y - \gamma)$
y = dimensionless temperature
z = axial direction

Greek letters

β = dimensionless heat transfer parameter (modified Stanton number)
γ = temperature sensitivity parameter
η = dimensionless radial direction, $= \xi^2$
ξ = dimensionless radial direction
μ = viscosity
π = dimensionless pressure
ρ = density
Φ = combined parameter
Λ = combined parameter

Subscripts

L = at outlet of tube
w = at wall of tube
z = at axial position z
0 = at inlet of tube
1 = at outlet of tube

Literature Cited

Davis, S. H., A. Kriegsmann, R. L. Laurence, and S. Rosenblat, "Multiple Solutions and Hysteresis in Steady Parallel Viscous Flow," *Phys. Fluids*, **26**, 1177 (1983).

Finlayson, B. A., *Nonlinear Analysis in Chemical Engineering*, McGraw-Hill, New York (1980).

Gupalo, Y. P., and S. Rayazantsev, "Thermochemical Instability in Steady Operating Regime of Continuous Flow Chemical Reactor with Fixed Catalyzer Bed," Akad. Nauk. SSSR, *Mekh. Zhidk. Gaza.*, 3(2), 64 (1968).

Kearsley, E. A., "The Viscous Heating Correction for Viscometric Flows," *Trans. Soc. Rheol.*, **6**, 253 (1962).

Kubicek, M., and M. Marek, *Computational Methods in Bifurcation Theory and Dissipative Structures*, Springer, New York (1983).

Lee, J. L., V. Balakotaiah, and D. Luss, "Thermoflow Multiplicity in a Packed-Bed Reactor. I: Adiabatic Case," *AIChE J.*, **33**, 1136 (1987).

———, "Thermoflow Multiplicity in a Packed-Bed Reactor. II: Impact of Volume Change," *AIChE J.*, **34**, 37 (1988).

Martin, B., "Some Analytical Solutions for Viscometric Flows of Power Law Fluids with Heat Generation and Temperature-Dependent Viscosity," *Int. J. Non-Linear Mech.*, **2**, 285 (1967).

Matros, Y. S., and N. A. Chumakova, "Multiplicity of Stationary Regimes in an Adiabatic Catalyst Layer," *Dokl. Akad. Nauk. SSSR*, **250**(6), 1421 (1980).

Meissner, J., "Deformationsverhalten der Kunststoffe im fluessigen und festen Zustand," *Kunststoffe*, **61**, 576 (1971).

Merzhanov, A. G., and A. M. Stolin, "Hydrodynamic Analogies of the Phenomena of Ignition and Extinction," *Zh. Tekh. Fiz*, **44**(1), 65 (1974).

Pearson, J. R. A., *Mechanics of Polymer Processing*, Elsevier, London (1985).

Pearson, J. R. A., Y. T. Shah, and E. S. A. Vieira, "Stability of Nonisothermal Flow in Channels. I: Temperature-Dependent Newtonian Fluid without Heat Generation," *Chem. Eng. Sci.*, **28**, 2079 (1973).

Pita, J., V. Balakotaiah, and D. Luss, "Thermoflow Multiplicity in a Packed-Bed Reactor: Conduction and Cooling Effects," *AIChE J.*, **35**, 373 (1989).

Shah, Y. T., and J. R. A. Pearson, "Stability of Nonisothermal Flow in Channels. II: Temperature-Dependent Power Law Fluids without Heat Generation," *Chem. Eng. Sci.*, **29**, 737 (1974a).

———, "Stability of Nonisothermal Flow in Channels. III: Temperature-Dependent Power Law Fluids with Heat Generation," *Chem. Eng. Sci.*, **29**, 1485 (1974b).

Villadsen, J., and M. Michelsen, *Solution of Differential Equations Models by Polynomial Approximation*, Prentice-Hall, Englewood Cliffs, NJ (1978).

Witmer, G., V. Balakotaiah, and D. Luss, "Finding Singular Points of Two-Point Boundary Value Problems," *J. Comput. Phys.*, **65**(1), 244 (1986).

Appendix A

Witmer et al. (1986) describe a method of finding singular points of two-point boundary value problems. We differentiate Eqs. 14 and 15 with respect to U to get at the collocation points

$$\frac{\partial^2 \pi}{\partial x \partial U} = 2^{n-2} \frac{\partial^2}{\partial \eta \partial U} \left(X_j \eta^{n+1/2} \frac{\partial u_j}{\partial \eta} \left| \frac{\partial u_j}{\partial \eta} \right|^{n-1} \right) \tag{A1}$$

$$\frac{\partial^2 y_i}{\partial x \partial U} = \frac{\partial}{\partial U}\left\{\frac{2\beta}{Bi\, u_i}\left[\frac{\partial}{\partial \eta}\left(\eta \frac{\partial y_i}{\partial \eta}\right) + Br\, X_i\, \eta^{(n+1)/2}\, 2^{n-1}\left(\frac{\partial u_i}{\partial \eta}\right)^2 \left|\frac{\partial u_i}{\partial \eta}\right|^{n-1}\right]\right\} \quad \text{(A2)}$$

$$\frac{\partial^3 \pi}{\partial x \partial U^2} = 2^{n-2}\frac{\partial^3}{\partial \eta \partial U^2}\left(X_j\, \eta^{(n+1)/2}\frac{\partial u_j}{\partial \eta}\left|\frac{\partial u_j}{\partial \eta}\right|^{n-1}\right) \quad \text{(A3)}$$

$$\frac{\partial^3 y_i}{\partial x \partial U^2} = \frac{\partial^2}{\partial U^2}\left\{\frac{2\beta}{Bi\, u_i}\left[\frac{\partial}{\partial \eta}\left(\eta \frac{\partial y_i}{\partial \eta}\right) + Br\, X_i\, \eta^{(n+1)/2}\, 2^{n-1}\left(\frac{\partial u_i}{\partial \eta}\right)^2 \left|\frac{\partial u_i}{\partial \eta}\right|^{n-1}\right]\right\} \quad \text{(A4)}$$

where $i = 1,2,\ldots,2M$, $j = 1,2,\ldots,N$.

These equations must be solved simultaneously with the original equations to get the first and second derivatives of π_1 with respect to U. At the cusp points these derivatives vanish. We approximate the first and second derivatives of u and y with respect to U by polynomials as in Eqs. 18 and 20. To determine the unknown constants of the polynomial approximations we use Eqs. A1 and A3 at the collocation points together with the first two derivatives of Eq. 16 (Gauss-Jacobi quadrature relation)

$$\sum_{k=1}^{N+1}\frac{\partial u_k}{\partial U} w_k = 0 \text{ and } \sum_{k=1}^{N+1}\frac{\partial^2 u_k}{\partial U^2} w_k = 0 \quad \text{(A5)}$$

to get a system of equations as described in the section on numerical solution of the model. The boundary conditions for the integration of Eqs. A1, A2, A3, and A4 are given by

$$\frac{\partial \pi}{\partial U} = 0, \frac{\partial^2 \pi}{\partial U^2} = 0, \frac{\partial y_i}{\partial U} = 0 \text{ and } \frac{\partial^2 y_i}{\partial U^2} = 0 \text{ at } x = 0 \quad \text{(A6)}$$

Appendix B

To prove that the insulated tube with constant radial temperature model cannot have multiplicity, we divide the momentum balance, Eq. 28, by the energy balance, Eq. 35, to get

$$\frac{d\pi}{dy} = -\frac{Bi}{4\beta\, Br} \quad \text{(B1)}$$

We integrate Eq. B1 and use boundary conditions 10a and 10b to get a linear relation between π and y

$$\pi = -\frac{Bi}{4\beta\, Br} y + \left(\frac{Bi}{4\beta\, Br} + 1\right) \quad \text{(B2)}$$

It follows from Eq. B2 that multiplicity is only possible if the same $y(1)$ exists for different U, because there exists a unique relation between y and π.

Now we show that the temperature profiles for different U cannot intersect except at $x = 0$. The energy balance, Eq. 35, is of the form

$$\frac{dy}{dx} = C_3\, X(y)\, U^n \quad \text{(B3)}$$

where $X(y)$ is a monotonic decreasing function of x (as no cooling exists, the temperature has to increase in the x direction due to heat dissipation). Because of the boundary condition, $y = 1$ at $x = 0$, $X(y)$ is the same for all the velocities U at $x = 0$. Thus, in a small neighborhood around $x = 0$ the slope of dy/dx increases with U^n. It follows that close to $x = 0$ the temperatures for larger U are higher than those for smaller U. If the temperature profiles for different U intersect somewhere, the one with the larger U must have a smaller slope at the intersection point because it comes from above. At the intersection point both profiles have the same temperature and therefore $X(y)$. But dy/dx is larger for the profile with the larger U, Eq. B3, and this leads to a contradiction. Therefore, temperature profiles for different U cannot intersect and multiplicity is not possible for the insulated tube with constant radial temperature model.

Manuscript received Aug. 21, 1989, and revision received Dec. 27, 1989.